#### Research Article

Yan Yan, Zhiquan Xing\*, Xilong Chen, Zhen Xie, Jiawei Zhang, and Yu Chen\*

# Axial compression performance of CFST columns reinforced by ultra-high-performance nano-concrete under long-term loading

https://doi.org/10.1515/ntrev-2022-0537 received November 30, 2022; accepted March 21, 2023

Abstract: The addition of nano-silica to ultra-high-performance concrete (UHPC) to increase its toughness has been proposed to obtain ultra-high-performance nanoconcrete (UHPNC). This work mainly studies the reinforcement effect of UHPNC on concrete filled steel tube (CFST) columns under long-term load. Ten CFST columns strengthened with UHPNC were selected and reinforced with UHPNC. The influences of different thicknesses of UHPNC reinforcement layer and different nano-silica contents on the axial compression properties of specimens were mainly studied, by loading specimens in two steps: long-term load and ultimate load. This study discussed the failure modes, compressive toughness, ultimate bearing capacity, initial stiffness, and ductility coefficient of the specimens. The results show that the outsourced UHPNC reinforcement method is an effective method to improve the performance of CFST columns during service period. With the increase in the thickness of UHPNC reinforced layer, the ultimate bearing capacity of CFST column increases greatly. The compression toughness is increased with the increase in nano-silica content and UHPNC reinforcement layer thickness. The decrease rate of initial stiffness increases with the increase in nano-silica content.

Yan Yan, Xilong Chen, Zhen Xie: State Grid Fujian Economic Research Institute, Fuzhou, 350013, China

Jiawei Zhang: College of Civil Engineering, Fuzhou University, Fuzhou, 350116, China

ORCID: Zhiquan Xing 0000-0003-2202-5738

**Keywords:** long-term load, axial compression performance, ultra-high-performance nano-concrete, nano-silica content, ultimate bearing capacity, failure mode

## 1 Introduction

In recent decades, the traditional concrete prevented the construction industry from moving forward due to its low strength of extension, poor stiffness, weak crack resistance, etc. In order to overcome these disadvantages, many scholars have conducted in-depth research on ordinary concrete over the years. In the 1970s, scholars first obtained concrete with compressive strength over 60 MPa [1]. At the same time, some scholars believe that the low strength of traditional concrete is due to the existence of natural pores between coarse aggregates, and adding fiber can enhance the stiffness of concrete [2]. In 1993, Richard and Cheyrezy first proposed the reactive powder concrete (RPC) [3]. The main feature is to apply pressure and increase density to improve stiffness during concrete solidification [4]. With further research by scientists, in 1994, De and Sedran [5] put forward the general idea of ultra-high-performance concrete (UHPC) [6,7]. In a sense, RPC could be regarded as a form of UHPC. The compressive strength of UHPC could go beyond 150 MPa, it is much stronger than ordinary concrete [8,9]. The principle of UHPC to obtain ultra-high strength and durability was to reduce the internal defects (pores and cracks) of the material by improving the fineness and activity of internal components and not using coarse aggregate [10–14]. The key factor to produce UHPC was to improve the micro and macro performance of its mixed components to ensure its dense granular filler [15-17].

So far, nanotechnology has been recognized as a major interdisciplinary product. The rich interdisciplinary development broadens the application field of nanotechnology. Li *et al.* [18] introduced low-dimensional nanometer structure photodetector (PD) and mixed PD,

<sup>\*</sup> Corresponding author: Zhiquan Xing, College of Civil Engineering, Fuzhou University, Fuzhou, 350116, China; International and Hong Kong, Macao and Taiwan Joint Laboratory of Structural Engineering, Fuzhou University, Fuzhou, 350116, China,

e-mail: 220525041@fzu.edu.cn, tel: +86 13645094982

<sup>\*</sup> Corresponding author: Yu Chen, College of Civil Engineering, Fuzhou University, Fuzhou, 350116, China; International and Hong Kong, Macao and Taiwan Joint Laboratory of Structural Engineering, Fuzhou University, Fuzhou, 350116, China, e-mail: yuchen@fzu.edu.cn, tel: +86 18030219629

analyzed their typicality, and got a lot of new results. Pawlowski et al. [19] made use of the hot silver plating method of nano silver based coatings and proposed that this method could replace the electrochemical method to a large extent. Zhang [20] conducted research on nanotubes and broadened the application of kaolin nanotubes. Recently, nano-concrete has also received more and more attention. This also drives the use of nanotechnology in infrastructure. Many scholars mixed nanomaterials with concrete to obtain better performance of modified concrete. And the nano-silica concrete used in this study is one of them. Adding nano-silica to concrete can make it more compact, increase the strength in the early stage, enhance the toughness, and significantly improve the durability of concrete [21]. At present, the construction industry has entered a critical period focusing on strengthening and reconstruction. However, the conventional reinforcement methods of concrete structures have some drawbacks in both. When welding reinforcement is used, the high temperature action makes the organization and performance of the welding parts deteriorate, causes weld defects and residual stress in the welding structure, and welding makes the structure form a continuous hole, and once the crack instability expands, it is possible that it breaks in the end, causing major accidents. The use of bolt connection needs to open holes in the base metal near the damage site, which weakens the section and forms a new stress concentration area. Ordinary bolts are easy to loosen under dynamic load, and high-strength bolts are easy to have stress relaxation, which reduces the repair effect of structure. When steel bonding technology is used, the structural adhesive should be used on the surface of the steel structure to stick the steel plate and rely on the structural adhesive to make it work together as a whole to improve the bearing capacity of the structure. These strengthening methods also have common shortcomings: the structural weight increase is larger, the steel plate is not easy to make into a variety of complex shapes, transportation and installation is not convenient, and the steel plate is easy to rust, affect the bonding strength, and high maintenance costs. Ultra-high-performance nano-concrete (UHPNC) has been partially applied in the field of maintenance reinforcement with its excellent mechanical properties and durability.

The UHPNC reinforced normal concrete not only had the advantages of simple technology and reliable stress but also conquered some shortcomings of traditional reinforcement methods, such as long construction periods, long curing time, and the weak contact surface between new and old concrete. In addition, compared to traditional concrete filled steel tube (CFST) columns,

UHPNC-wrapped CFST columns can be used as an attractive alternative to buildings at risk of corrosion or fire, as it protects the components of existing buildings. No experimental research has been conducted by scholars in the field of reinforcement of new materials. Most scholars still use outsourced UHPC for reinforcement, and the actual operation process of the two is similar. Genedy [22] used a CFRP plate and UHPC to strengthen the T-shaped beams. It is found that the bearing capacity after reinforcement is very high. In order to study the applicability of strengthening the existing concrete structures with UHPC, Katrin et al. [23] studied the flexural performance of 12 fullscale test beams and found that the tensile zone of concrete beams strengthened with UHPC could improve the flexural bearing capacity and cracking load of the beams. Prem et al. [24] adopted UHPC to strengthen the damaged test beam and found that the bearing capacity of the strengthened beam was greatly increased. Lampropoulos et al. [25] studied the mechanical properties of UHPC reinforced concrete beams and established a finite element model to simulate the test. Al-Osta et al. [26] studied the influence of UHPC-strengthened concrete beams on their flexural performance. Some specimens were strengthened in situ, while other specimens were connected with prefabricated UHPC plates through structural adhesives. The bearing capacity of UHPC-reinforced beam has been greatly improved. Even if the concrete surface was not treated in advance, UHPC and concrete still had strong bonding ability. Beschi et al. [27] strengthened the beam-column joints with UHPC. Finally, it is found that this method significantly improves the bearing capacity of nodes. Lee and Huang [28] used UHPC to strengthen concrete structures in different extreme environments and found that UHPC not only had excellent mechanical properties, but also had excellent durability and strong adaptability to extreme environments. Tayeh et al. [29] found that the bonding ability between the UHPC strengthening layer and the old concrete was good, and the impermeability of the strengthened contact surface was also greatly improved. In addition, Huang et al. [30] studied the influence of the combined use of nanomaterials and steel fibers on the processability, compressive strength, and microstructure of UHPC. Luo et al. [31] used the continuously synthesized graphene oxide to improve the bending strength of UHPC. Liu et al. [32] studied the application of nanomaterials in UHPC.

With its excellent mechanical properties and excellent durability, UHPNC has a great advantage over common concrete reinforcement methods. However, the basic research of UHPNC is not deep enough, and the application research of UHPNC in the field of reinforcement is far from enough. Foreign scholars [33–37] have conducted some studies on

the application of UHPC in the field of reinforcement, and their experimental results can provide reference for our future research. It is worth noting that there are few research works on the reinforcement and maintenance of UHPNC at present, especially on the reinforcement under long-term load. The main damage characteristics of CFST columns under long-term continuous loading were investigated. The reinforcement of the existing structure must be carried out under the load state, the reinforcement of the columns in the building must be carried out under the load of the floor, and the reinforcement of the pier must be carried out under the load of the bridge. Therefore, it is very necessary to study the reinforcement of CFST columns under long-term load. To further investigate the effectiveness of UHPNC-reinforced building component, this study focuses on the axial compression performance of the UHPNC-reinforced CFST column.

# 2 Experimental research

### 2.1 Specimen design

In this experiment, the CFST square column was strengthened by UHPNC under long-term load, and the axial compression test was conducted. The specimens could be loaded in two steps: long-term sustained load and ultimate load. There are ten specimens in total, one of the specimens is the control specimen which is not strengthened under long-term load. The self-made test device of long-term continuous load is shown in Figure 1, the other

specimens are UHPNC-reinforced CFST column with the same load and load-holding time as the control group, with different UHPNC reinforcement layer thickness (T) and nano-silica content (D). Details of the specimen are shown in Figure 2. As shown in the figure, after the ordinary concrete-filled steel tube column is made, the outer side of the steel tube should be welded with round head stud. The length of the round head stud should be 80% of the thickness of the reinforcement layer. After the stud is welded, the customized template should be bound on it and UHPNC can be poured under long-term load. The creep deformation of CFST columns under long-term continuous loads was largely completed within 90 days and remained largely unchanged after 200 days. In this test column, the load was held for 200 days under the condition of long-term constant load of 550 kN [38]. The built-in force sensor was used to detect the constant axial load. When the load holding time was reached, the UHPNC was reinforced after pouring. Finally, the UHPNC was solidified and the specimen was moved to the ultimate loading test device.

The purpose of this experiment is to research the effect of different thicknesses of UHPNC-reinforced layer [39] and nano-silica [40] content on the bearing capacity of CFST column under long-term continuous load. The CFST column is made of concrete with a strength of 30 MPa, and the square steel tube size is 120 mm  $\times$  120 mm  $\times$  360 mm. The parameter variables of each specimen in this test are shown in Table 1. In the Table, the CFST represents the rectangular concrete-filled steel tube column, T (thickness) is the thick gauge of UHPNC reinforcement layer, and D (dosage) is the nano-silica content. According to the density calculation formula, the

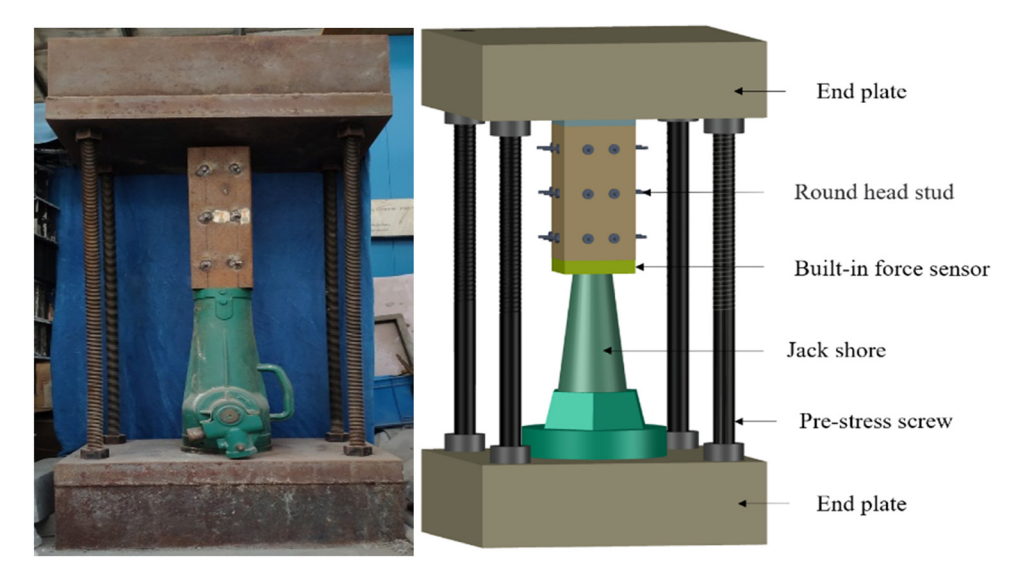


Figure 1: Long-term load testing device.

4 — Yan Yan et al. DE GRUYTER

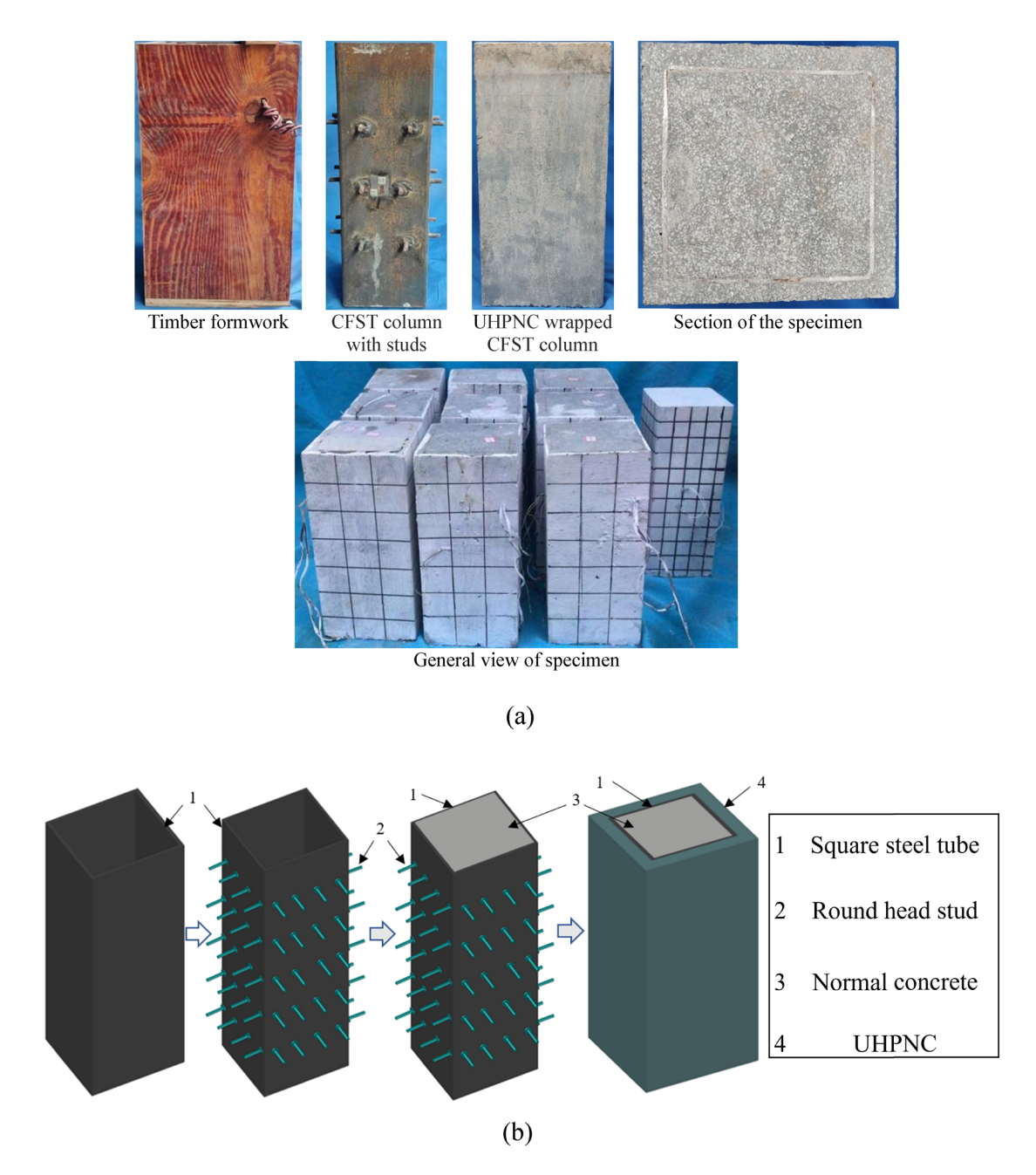


Figure 2: The details of CFST columns strengthened with UHPNC. (a) Sample pouring process and general picture. (b) Flow chart of specimen pouring.

number of kilograms of nano-silica required for 1 cubic meter of super-high-performance nano-concrete can be calculated by multiplying by one percent.

#### 2.2 Material properties

All test specimens were fabricated at the prefabrication yard of Fuzhou University, and UHPNC-reinforced columns were completed under pressure during the fabrication process. 30 MPa is the design strength of concrete and the mix is shown in Table 2. The UHPNC is composed of cement, fine sand, nano-silica fume, steel fiber, water, and water reducer in a certain proportion, as shown in Figure 3. The specific mix proportion of UHPNC is presented in Table 3. Three concrete cubes were used for each kind of concrete to obtain the compressive strength  $f_{\rm cu}$ . The size of ordinary concrete cube test block is 150 mm  $\times$  150 mm  $\times$  150 mm, UHPNC cube test block size is 100 mm  $\times$  100 mm  $\times$  100 mm. And the

Table 1: List of specimen parameters

Specimen label	Normal concrete strength (MPa)	<i>T</i> (mm)	<b>D</b> (%)	Long-term load value (kN)	Load holding time (Day)	Type of reinforcement	Specimen size (mm)
CFST-T10-D1	30	10	1	550	200	Square	130 × 130 × 360
CFST-T15-D1	30	15	1	550	200	Square	$135\times135\times360$
CFST-T20-D1	30	20	1	550	200	Square	$140\times140\times360$
CFST-T10-D2	30	10	2	550	200	Square	$130\times130\times360$
CFST-T15-D2	30	15	2	550	200	Square	$135\times135\times360$
CFST-T20-D2	30	20	2	550	200	Square	$140\times140\times360$
CFST-T10-D3	30	10	3	550	200	Square	$130\times130\times360$
CFST-T15-D3	30	15	3	550	200	Square	$135\times135\times360$
CFST-T20-D3	30	20	3	550	200	Square	$140\times140\times360$
CFST-T0-D0	30	_	_	550	200	_	$120\times120\times360$

Table 2: Mix proportion of C30 concrete

Cement (kg/m³)	Water (kg/m³)	Sand (kg/m³)	Coarse aggregate (kg/m³)
461	175	512	1,250

concrete used in the test is cured in the same environment as the components, and the specific performance is shown in Table 4. Q235 square steel tube was used in this test. The steel tube thickness is 2.75 mm. To accurately obtain the steel material properties, the tensile

test was carried out according to (GB/T228.1-2010). The obtained yield strength  $(f_v)$ , ultimate tensile strength  $(f_{\rm u})$ , etc., are shown in Table 5.

#### 2.3 Test process

Combined with the load and size required for loading specific specimens and the existing test equipment in the School of Civil Engineering of Fuzhou University, 10,000 kN servo hydraulic press was selected to carry out the limit loading after load holding, LVDTs are arranged in the

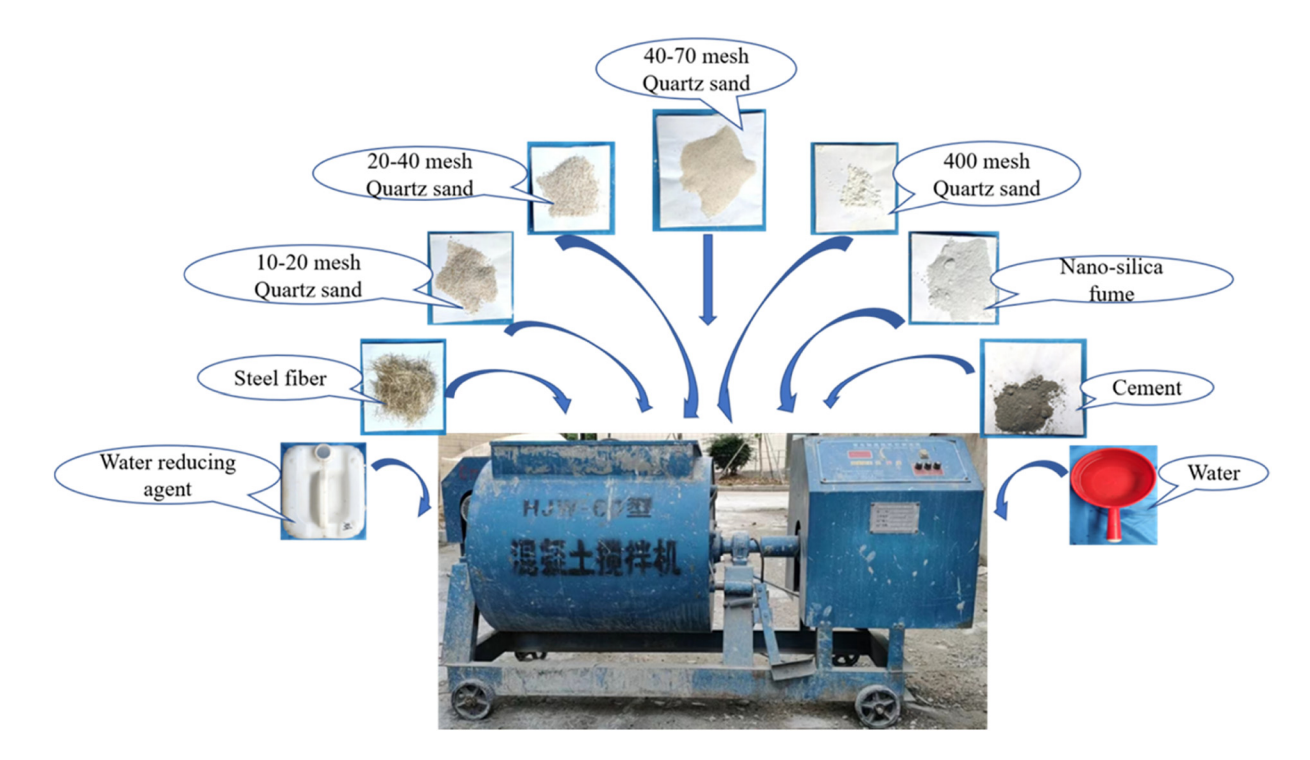


Figure 3: Composition of UHPNC and mixing device.

Table 3: UHPNC mix proportion

Cement (kg/m³)	Steel fiber (kg/m³)	<b></b>		and (kg/m³)		Water reducing	Water	Nano-silica
		40-70 mesh	20-40 mesh	10-20 mesh	400 mesh	agent (kg/m³)	(kg/m³)	fume (kg/m <sup>3</sup> )
844.5	253.4	118.2	346.3	447.6	79.4	21.1	241.5	78 (1%) 156 (2%) 234 (3%)

Table 4: Performance test results of concrete cube material

D (%)	Serial number	Cubic compressive strength $(f_{cu}/MPa)$	Average value $(f_{cu}/MPa)$
0 (normal	No. 1	34	32
concrete)	No. 2	32	
	No. 3	30	
1 (UHPNC)	No. 1	115	114
	No. 2	111	
	No. 3	116	
2 (UHPNC)	No. 1	120	121
	No. 2	124	
	No. 3	119	
3 (UHPNC)	No. 1	127	125
	No. 2	124	
	No. 3	124	

position as shown in Figure 4 and built on both sides of the component to test its vertical displacement. A pair of longitudinal and transverse strain gauges are arranged at the centroid of a square CFST column, and a pair of longitudinal and transverse strain gauges are arranged on each side of one of its edges. The reinforced specimens are arranged with a pair of longitudinal and transverse strain gauges on each of the four surfaces as exhibited in Figure 4. To make the full section of the test piece uniformly compressed, before the test loading, grind the loading surface with gypsum, apply a force of 20 kN to the test specimen, and hold the load for 20 min to ensure gypsum solidification. In the formal loading, the axial compression test is first carried out by means of hierarchical loading. Before reaching 70% of the estimated ultimate

load, loading at the speed of 0.5 kN/s, the load value is about 1/10 of the estimated ultimate load, and the loading time of each stage lasts for 2–3 min. When the load value exceeds 70% of the estimated ultimate load, the load of each stage is about 1/30 of the estimated ultimate load. The test was stopped until the applied axial load dropped to 85% of the ultimate load or the axial strain exceeded 0.15.

#### 3 Test result

#### 3.1 Failure modes

According to the failure characteristics of UHPNC-reinforced CFST column under load condition, the failure mode of CFST column was discussed. The failure mode is presented in Figure 5. The results show that the failure process of the initial stage is similar to that of ordinary concrete columns under axial load. The axial deformation of the specimen increased linearly with the increase in the applied loading. And then the axial deformation increased faster than that of the applied loading growth rate. When the applied loading approaches the peak load, the "sizzling" sound of steel fiber pulling out of UHPNC could be heard. When the applied load reached the peak load, the louder sound of "Bang" could be heard. The bearing capacity of the specimen showed a linear decline. The UHPNC reinforcement layer was peeled off the specimen. Although the nano content is different, the failure mode is UHPNC layer shedding, so the component can be considered as failure. After the specimen failed, it could be

Table 5: Results of steel properties

Test coupons	Yield strength $(f_y/\text{MPa})$	Average value $(f_y/\text{MPa})$	Ultimate tensile strength $(f_u/\text{MPa})$	Average value $(f_u/MPa)$
No. 1	240	243	428	432
No. 2	244		435	
No. 3	245		433	



Figure 4: Test specimen under compressive loading.

found that the core concrete of the specimen was compressed. The UHPNC reinforcement layer was peeled off, and the steel tube was significantly deformed. This is mainly because the limit load-bearing capability state of the UHPNC wrapped CFST column was mainly contributed by the UHPNC reinforcement layer. Therefore, the specimen finally shows the failure when the UHPNC reinforcement layer peeled off.

#### 3.2 Load-displacement curves

The loading and corresponding displacement data collected by the data system of the test device were obtained, and the load—displacement curve of the specimen is shown in Figure 6. In this figure, the vertical axis P is the axial load and the horizontal axis  $\Delta$  is the corresponding displacement value. Before the yielding of the test specimen, the displacement increases linearly with the increase in the applied load. When the applied loading was close to the peak load, the corresponding displacement increase rate was greater than the increased rate of the applied loading. Then, the applied loading decreased quickly with a little displacement increase. These load—displacement curves indicated that most specimens were mainly in brittle failure mode under the test. The ultimate bearing capacity ( $N_{\rm u}$ ) of the specimen partially increases with the content of nano-silica. With the increase in the thickness of UHPNC reinforcement layer, the increase rate increases greatly. Among other things,

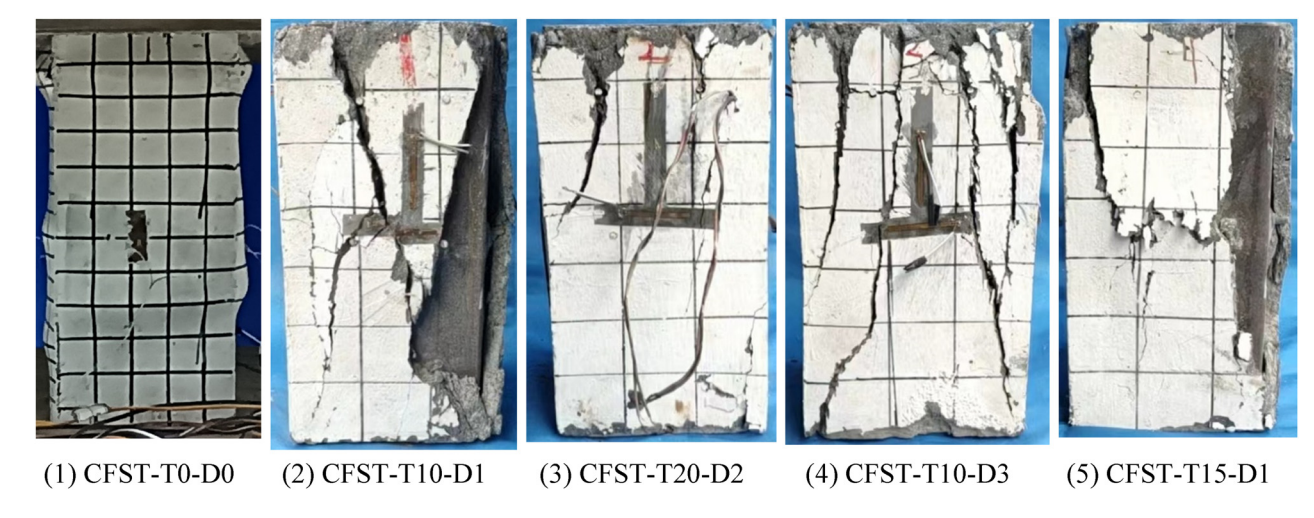


Figure 5: Failure mode of specimens under axial compressive loading.

8 — Yan Yan et al. DE GRUYTER

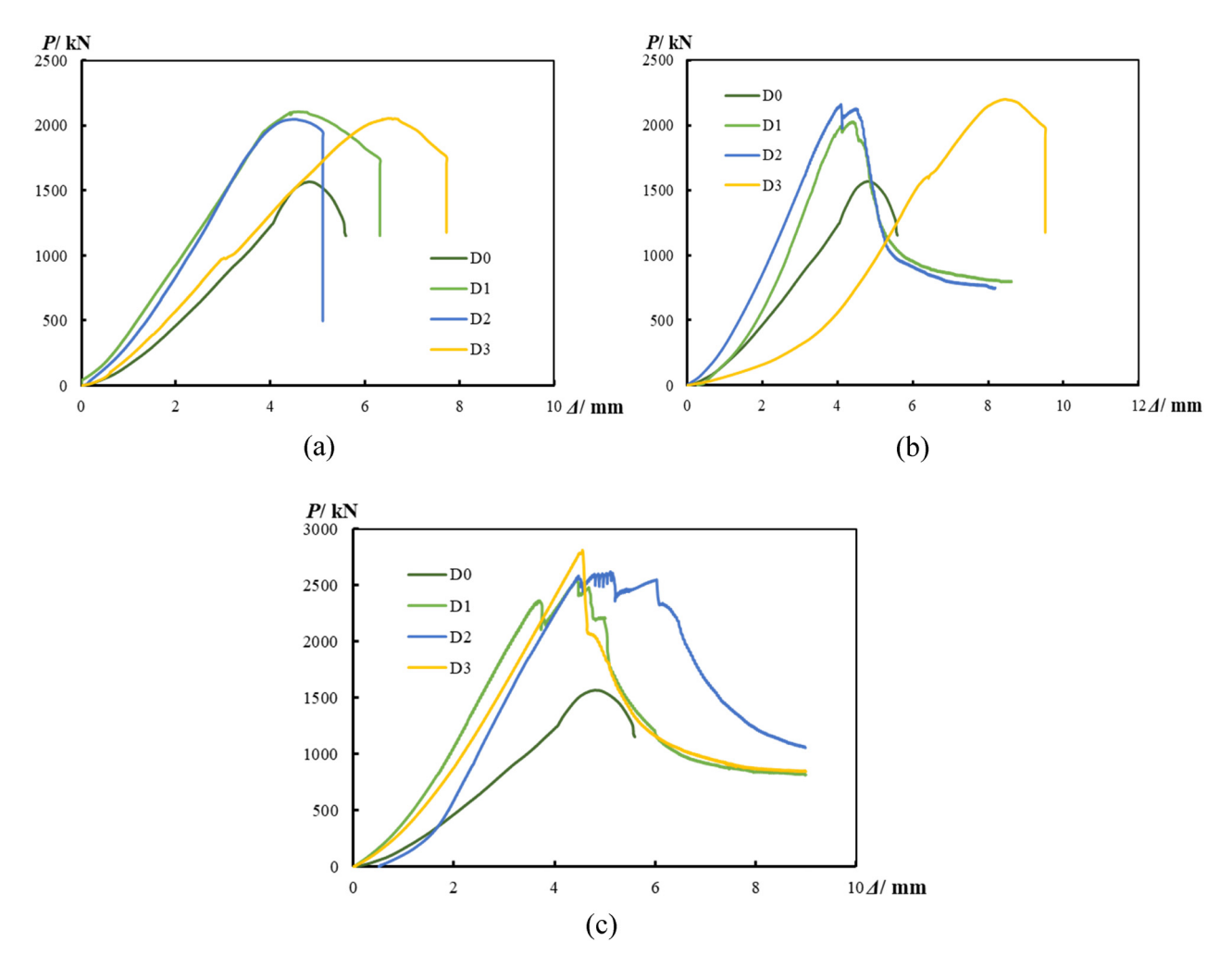


Figure 6: Load-displacement curve of CFST column reinforced by UHPNC. (a) CFST-T10, (b) CFST-T15, and (c) CFST-T20.

Table 6: Test results of specimen

Specimen label	Ultimate bearing capacity (kN)	Ultimate displacement (mm)	Yield capacity (kN)	Yield displacement (mm)	Initial stiffness (kN/mm)	Ductility coefficient	Compression toughness (kN mm)
CFST-T10-D1	2105.80	4.59	1684.61	3.39	451.53	1.36	5031.35
CFST-T15-D1	2027.72	4.39	1622.17	3.48	316.69	1.26	3710.74
CFST-T20-D1	2544.64	4.44	2035.71	3.19	499.23	1.39	5609.14
CFST-T10-D2	2048.40	4.5272	1638.72	3.2896	401.89	1.38	4512.08
CFST-T15-D2	2162.54	4.10	1730.03	3.30	410.64	1.24	4733.03
CFST-T20-D2	2621.70	5.11	2093.58	3.80	382.33	1.35	5926.74
CFST-T10-D3	2055.20	6.54	1644.16	4.88	304.28	1.34	6818.32
CFST-T15-D3	2200.02	8.45	1760.02	6.88	168.99	1.23	7451.22
CFST-T20-D3	2812.77	4.55	2250.22	3.82	455.77	1.19	5339.22
CFST-T0-D0	1564.75	4.89	1251.82	4.10	244.22	1.19	3309.94

the ultimate bearing capacity P(x) and compressive toughness (CT) were obtained from the load–displacement curves which were used to analyze the compressive performance of

the test specimen, as shown in Table 6. The follow-up will also be a detailed introduction to compressive toughness, which will not be described here.

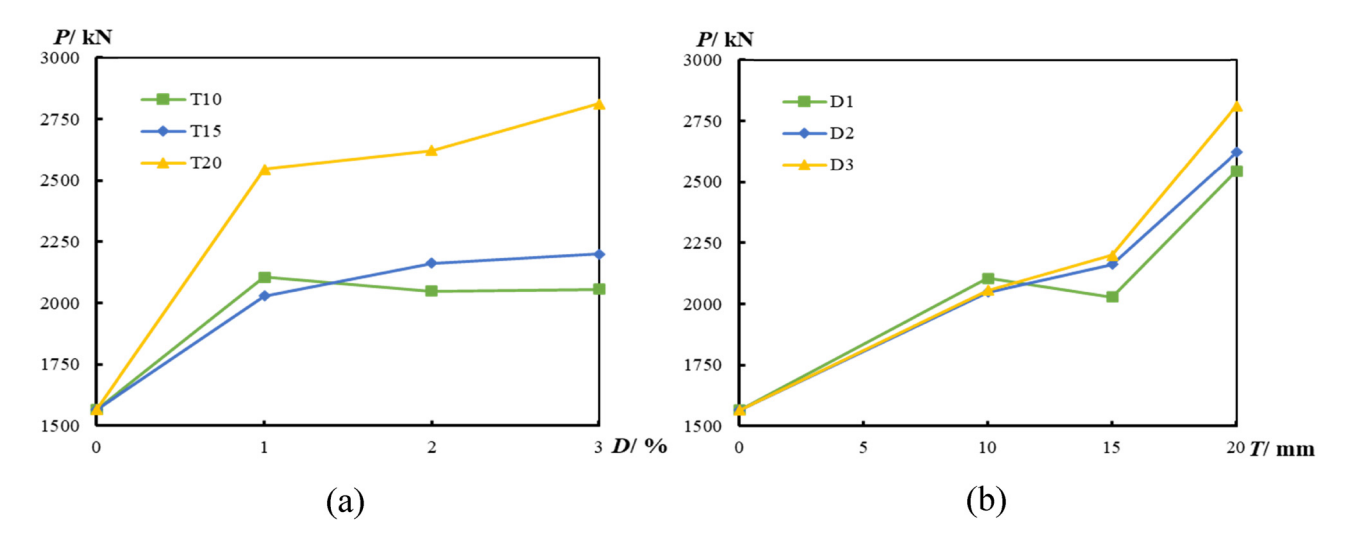


Figure 7: Influence of test variables on ultimate bearing capacity. (a) Influence of nano-silica content and (b) influence of thickness of UHPNC reinforcement layer.

#### 3.3 Ultimate bearing capacity

The influence of nano-silica content in the UHPNC-reinforced layer on the ultimate bearing capacity of CFST column after use is shown in Figure 7. It can be obviously found that the ultimate bearing capacity of CFST column is greatly improved due to the existence of UHPNC reinforcement layer. For example, when the thickness of UHPNC-reinforced layer reaches 10 mm and the content of nano-silica is 1%, the ultimate bearing capacity of the specimen increases by 42% on average. The results show that this method is an effective method to improve the ultimate bearing capacity of CFST column in the service period. In addition, with the increase in nano-silica content, the ultimate bearing capacity of CFST column increased slightly during the service period. For example, when the nano-silica content was increased from 1 to 2% and from 2 to 3%, the ultimate bearing capacity of the test specimen increased by an average of 2 and 3%, respectively. It could be concluded that the ultimate bearing capacity of CFST columns was greatly affected by the UHPNC reinforcement layer. But the effects of nano-silica content on the ultimate bearing capacity were not obvious. However, when the thickness of UHPNC-reinforced layer is 20, the ultimate bearing capacity is greatly increased, and the role of nano-silica becomes obvious. It can be concluded that with the increase in the thickness of the reinforced layer, the nano content has an obvious effect on the ultimate bearing capacity. It also could be found that the increased rate of ultimate bearing capacity was greatly increased with the increase in UHPNC reinforcement layer thickness.

Figure 7 discusses the influence of the thickness of the UHPNC reinforcement layer on the ultimate bearing capacity of CFST under ultimate loading during the service period. With the increase in the thickness of the UHPNC reinforcement layer, the ultimate bearing capacity increases significantly. For example, when the nanosilica content was 2%, the ultimate bearing capacity of the test specimen increased from 2048.40 to 2162.54 kN and from 2162.54 to 2621.70 kN with the increase in UHPNC reinforcement layer thickness from 10 to 15 mm and from 15 to 20 mm, respectively. In general, when the UHPNC reinforcement layer thickness was increased from 10 to 15 mm and from 15 to 20 mm, the ultimate bearing capacity of the test specimen increased by an average of 3 and 25%, respectively. It indicated that the improvement rate of ultimate bearing capacity increased with the increase in UHPNC reinforcement layer thickness. The reason was that the stiffness of the UHPNC reinforcement layer increased with the increase in thickness. Therefore, the thicker UHPNC reinforcement layer could provide a more powerful constraint to the concrete-filled steel tubular column.

#### 3.4 Initial stiffness

The influence of the test parameters on the initial stiffness of the specimen is shown in Figure 8. It could be found that the initial stiffness of the test specimen was greatly increased because of the UHPNC reinforcement layer. For example, the initial stiffness of the test increased by an average of 73% when the UHPNC reinforcement layer was

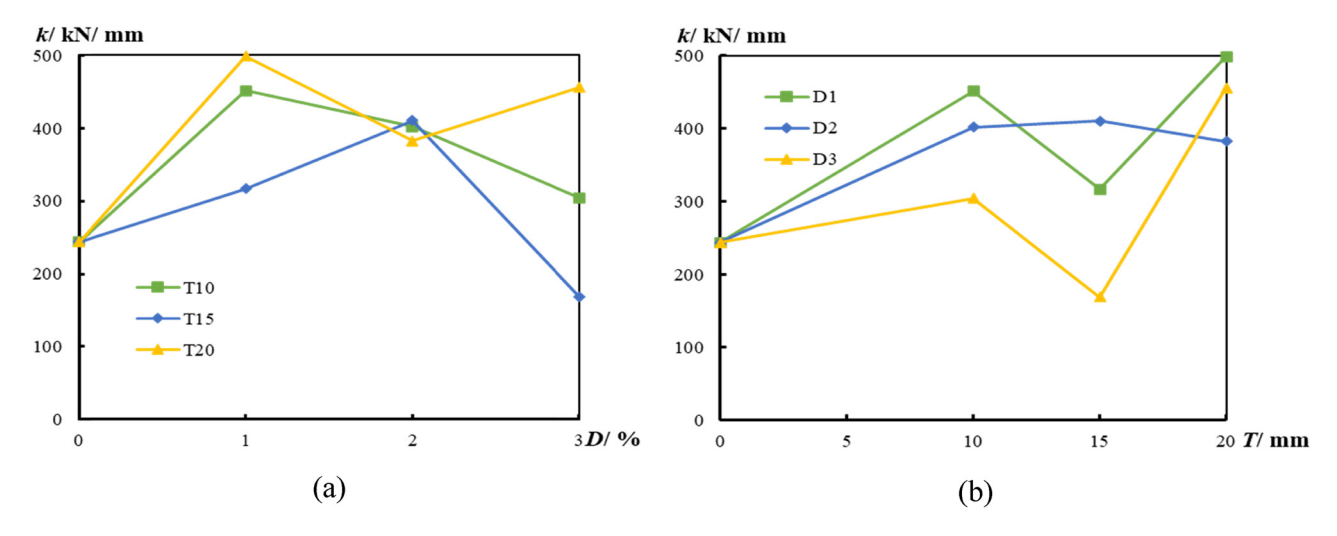


Figure 8: Influence of the test parameters on the initial stiffness of the specimen. (a) Influence of nano-silica content and (b) influence of UHPNC reinforcement layer thickness.

10 mm and the nano-silica content was 1%. The results show that this method is an effective measure to improve the initial stiffness of CFST column under long-term load. However, the initial stiffness of the test specimen decreased with the increase in nano-silica content. For example, when the UHPNC reinforcement layer thickness was 10 mm, the initial stiffness of the test specimen decreased from 451.53 to 401.89 kN/mm and from 401.89 to 304.28 kN/mm with the increase in the nano-silica content from 1 to 2% and from 2 to 3%, respectively. It could be found that the initial stiffness decrease rate increased with the increase in nano-silica content.

Figure 8 discusses the influence of the thickness of the UHPNC reinforcement layer on the initial stiffness of the specimen during the service period. It could be found that the initial stiffness of the test specimen increased with the increase in the UHPNC reinforcement layer thickness. For example, when the nano-silica content was 1%, the initial stiffness of test specimen increased from 451.53 to 499.23 kN/mm with the increase in UHPNC reinforcement layer thickness from 10 to 20 mm. And the initial stiffness increased from 304.28 to 455.77 kN/mm with the increase in UHPNC reinforcement layer thickness from 10 to 20 mm when the nano-silica content was 3%. The decrease rate of initial stiffness increases with the increase in nano-silica content.

#### 3.5 Ductility coefficient

The ultimate loading experiment results of CFST columns wrapped by UHPNC under long-term sustained load are shown in Table 6. Meanwhile, the value of ductility coefficient  $\mu$  is calculated according to formula (1).

$$\mu = \frac{\Delta_{\rm u}}{\Delta_{\rm y}},\tag{1}$$

where  $\Delta_u$  is the ultimate displacement and  $\Delta_y$  is the corresponding yield displacement [41].

Figure 9 discusses the influence of the nano-silica content in the UHPNC reinforcement layer on the ductility coefficient of CFST column during the service period. The ductility coefficient of test specimen increased because of the UHPNC reinforcement layer. For example, the ductility coefficient increased by an average of 12% when the UHPNC reinforcement layer was 10 mm and the nano-silica content was 1%. The results show that using UHPNC to wrap CFST column under long-term load is an effective method to improve the ductility coefficient of CFST column during service period. However, with the increase in nano-silica content, the ductility coefficient of UHPNC components decreases. For example, when the UHPNC reinforcement layer thickness was 20 mm, the ductility coefficient decreased from 1.394 to 1.345 and from 1.345 to 1.191 with the increase in nano-silica content from 1 to 2% and from 2 to 3%, respectively. In general, when the nanosilica content was increased from 1 to 2% and from 2 to 3%, the ductility coefficient decreased by an average of 1 and 5%, respectively. It indicated that the decrease rate of ductility coefficient increased with the increase in nano-silica. But, overall, the effect of nano-silica content on the ductility coefficient was not obvious.

#### 3.6 Compressive toughness

The compressive toughness is the value of the area under the load–displacement curve before the peak load. The

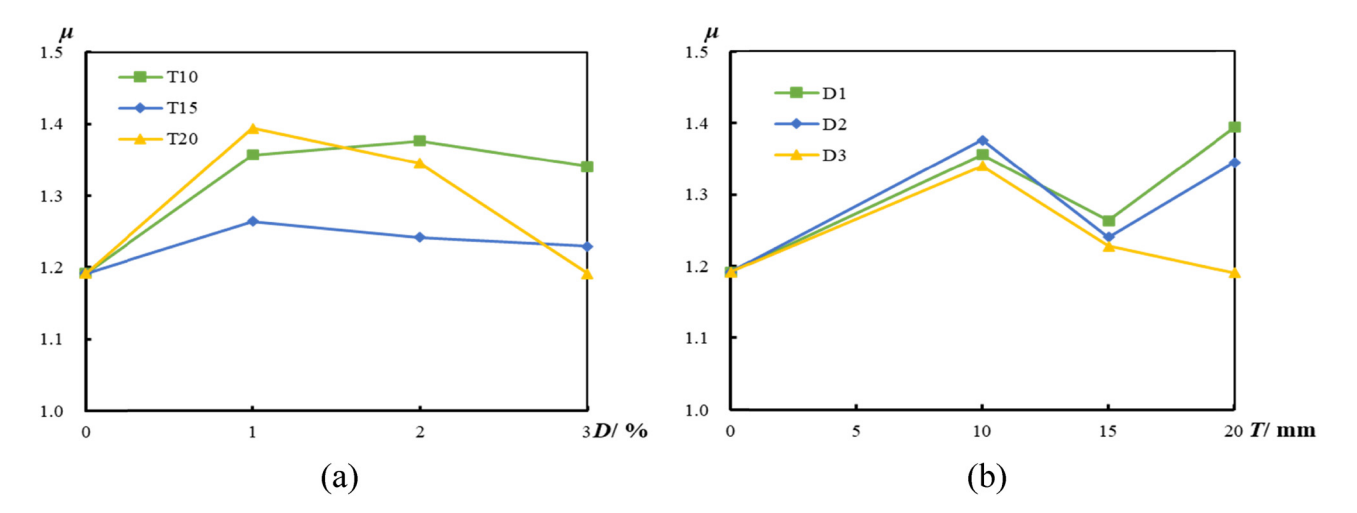


Figure 9: Influence of each test parameter variable on the ductility coefficient. (a) Influence of nano-silica content and (b) influence of UHPNC reinforcement layer thickness.

compression toughness represents the energy released when the UHPNC wrapped CFST column is damaged [42–45]. The compressive toughness can be calculated as follows:

$$CT = \int_{x=0}^{x=\Delta_{\text{max}}} P(x)dx,$$
 (2)

where  $\Delta_{\text{max}}$  is the displacement corresponding to the peak load.

The effects of nano-silica content on the compression toughness of test specimen are presented in Figure 10. It could be found that the compression toughness increased because of the UHPNC-reinforced layer. For example, the compression toughness increased by an average of 45% when the UHPNC reinforcement layer was 10 mm and the nano-silica content was 1%. In addition, the compression

toughness increased with the increase in nano-silica content, such that when the UHPNC reinforcement layer thickness was 15 mm, the compression toughness of the test specimen increased from 3710.74 to 4733.03 kN mm and from 4733.03 to 7451.22 kN mm with the increase in of nano-silica content from 1 to 2% and from 2 to 3%, respectively. The reason may be that more energy was needed to pull out the nano-silica from the fracture surface because of the increasing nano-silica content.

In Figure 10, the effects of UHPNC reinforcement layer thickness on the compression toughness were discussed. It could be found that the compression toughness increased with the increase in UHPNC reinforcement layer thickness. For example, when the nano-silica content was 2%, the compression toughness increased from 4512.08 to 4733.03 kN mm and from 4733.03 to 5926.74 kN

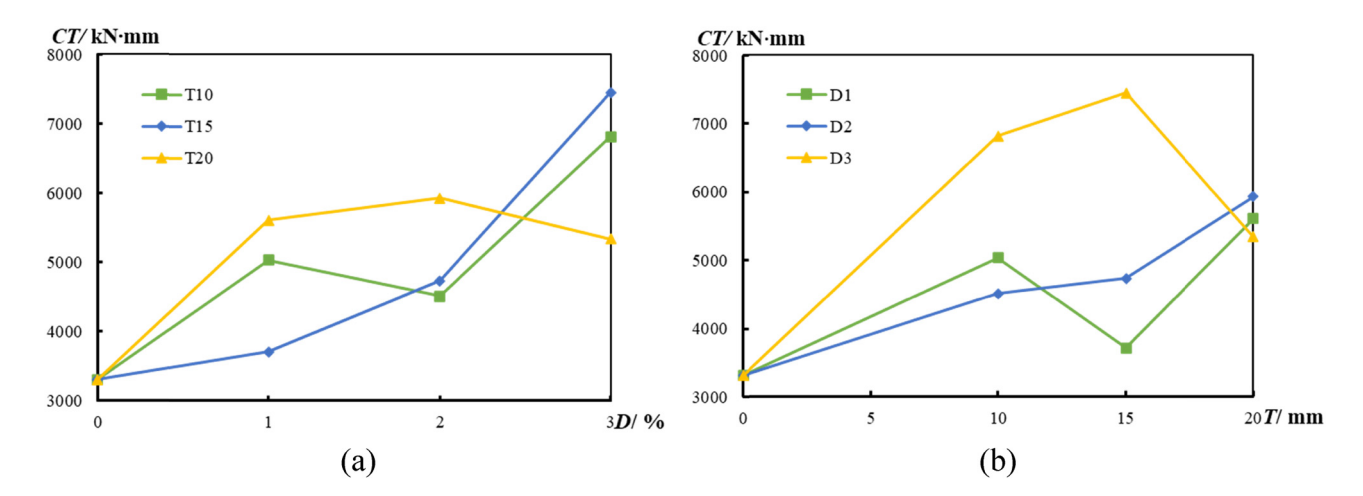


Figure 10: Influence of test variables on compressive toughness. (a) Influence of nano-silica content and (b) influence of UHPNC reinforcement layer thickness.

Table 7: Calculation results of ultimate bearing capacity of specimen
Table 7. Catediation results of attimate searing capacity of specimen

Specimen label	N <sub>u</sub> (kN)	N <sub>ue</sub> (kN)	<i>T</i> (mm)	<b>D</b> (%)	α	β	N <sub>uc</sub> (kN)	$N_{\rm uc}/N_{\rm u}$	Error (%)
CFST-T10-D1	2105.80	1950.02	10	1	1.0	1	1906.81	0.91	-9
CFST-T15-D1	2027.72	2305.70	15	1	1.5	1	2215.24	1.09	9
CFST-T20-D1	2544.64	2661.38	20	1	2.0	1	2511.53	0.99	-1
CFST-T10-D2	2048.40	1993.70	10	2	1.0	2	1929.47	0.94	-6
CFST-T15-D2	2162.54	2371.22	15	2	1.5	2	2252.32	1.04	4
CFST-T20-D2	2621.70	2748.74	20	2	2.0	2	2563.01	0.98	-2
CFST-T10-D3	2055.20	2018.66	10	3	1.0	3	1931.29	0.94	-6
CFST-T15-D3	2200.02	2408.66	15	3	1.5	3	2261.60	1.03	3
CFST-T20-D3	2812.77	2798.66	20	3	2.0	3	2578.04	0.92	-8
Mean value	_	_	_	_	_	_	_	0.98	-2
Variance	_	_	_	_	_	_	_	0.003	0.003

mm with the increase in UHPNC reinforcement layer thickness from 15 to 20 mm.

# 4 Formula to calculate ultimate bearing capability

A new comprehensive calculation method is used to calculate the ultimate bearing capacity ( $N_{\rm uc}$ ) of CFST column under axial compression load under long-term loading condition of UHPNC wrap. The effects of nano-silica content and UHPNC reinforcement layer thickness must be considered while calculating the ultimate bearing capacity. The ultimate bearing capacity of UHPN- reinforced columns subjected to axial compressive loading was calculated by introducing the influence coefficient ( $\eta$ ) of test parameters. The assumed functional forms of the calculation formula are as follows:

$$N_{\rm uc} = \eta \times N_{\rm ue},$$
 (3)

$$N_{\text{ue}} = N_{\text{ue1}} + N_{\text{ue2}},$$
 (4)

$$N_{\text{ue1}} = 1.3 \times (f_{\text{s}}A_{\text{s}} + f_{\text{c}}A_{\text{c}}),$$
 (5)

$$N_{\text{ue2}} = 1.3 \times (N_{\text{ue1}} + f_{\text{U}}A_{\text{U}}),$$
 (6)

$$\eta = -0.44 \times f(\alpha) \times f(\beta) + 1.49,\tag{7}$$

$$f(\alpha) = 0.08 \times \alpha + 1.12,\tag{8}$$

$$f(\beta) = 0.02 \times \beta + 0.95,\tag{9}$$

$$\alpha = \frac{T}{T_0}$$

$$\beta = \frac{D}{D_0},$$
(10)

where the  $A_s$ ,  $A_c$ , and  $A_u$  were the cross-sectional area of steel, normal concrete, and UHPNC, respectively.  $f(\alpha)$  and

 $f(\beta)$  are the functions of  $\alpha$  and  $\beta$ , respectively. The  $T_0$  was 10 mm and  $D_0$  was 1 (%).

The calculation value ( $N_{\rm uc}$ ) of the CFST column under UHPNC reinforcement is compared with the statistical results of the test value, which proves the rationality and accuracy of the formula. As can be seen from Table 7, the calculated limit capacity values of most specimens are smaller than those of the test results. The mean value is 0.98, and the variance is 0.03, which indicates that the equation is reasonable and accurate in predicting the ultimate bearing capacity of CFST column strengthened by UHPNC under load holding state.

# 5 Conclusion

The effects of UHPNC reinforcement layer thickness and nano-silica content on the compressive properties of CFST column under load holding condition were studied. This study discussed the failure modes, load—displacement curves, ultimate bearing capacity, initial stiffness, ductility coefficient, and compression toughness. The following conclusions are obtained from this study:

- The ultimate bearing capacity, initial stiffness, ductility coefficient, and compressive toughness of CFST column under load holding state are improved by UHPNC reinforcement layer. The results show that the outsourced UHPNC reinforcement method is an effective method to improve the performance of CFST columns during service period.
- 2) The ultimate bearing capacity of CFST column is greatly increased with the increase in UHPNC reinforcement layer thickness. And the improvement rate of ultimate bearing capacity is increased with the increase in UHPNC reinforcement layer thickness. However, the

- effect of nano-silica content on the ultimate bearing capacity is not obvious.
- 3) During the service period, the initial stiffness of CFST column increases with the increase in the thickness of UHPNC reinforcement layer and decreases with the increase in nano-silica content. The decrease rate of initial stiffness increases with the increase in nanosilica content.
- 4) The ductility coefficient of CFST column decreased with the increase in nano-silica content. And the decrease rate of ductility coefficient increased with the increase in nano-silica content. In addition, the compression toughness increases with the increase in nano-silica content and UHPNC reinforcement layer thickness.
- 5) According to the test results, a reasonable and conservative formula for calculating the ultimate compressive capacity of CFST column under long-term constant load reinforced by UHPNC is put forward. The calculated results are in good agreement with the experimental results.

**Funding information:** This research work was supported by National Natural Science Foundation of China (No. 52078138), the Guiding Project of Fujian Province (No. 2021Y0003), the Science and Technology Planning Project of Fuzhou (No. 2021-Y-083), The Fifth Batch of Science and Technology Plan Project of Housing and Urban-Rural Construction Industry of Fujian Province in 2022 (No. 2022-K-296), and Project of the twenty-eighth Undergraduate Scientific Research Training Program of Fuzhou University (No. 28130).

**Author contributions:** All authors have accepted responsibility for the entire content of this manuscript and approved its submission.

Conflict of interest: The authors state no conflict of interest.

# References

- Wu Z. Green high performance concrete the trend of concrete development. China Concr Cem Products. 1998;1:3-6.
- Chen BC, Ji T, Huang QW, Wu HZ, Ding QJ, Zhan YW. Review of research on ultra-high performance concrete. J Archit Civ Eng. 2014;31(3):1-24.
- Richard P, Cheyrezy M. Composition of reactive powder concretes. Cem Concr Res. 1995;25(7):1501-11.

- Li Y, Xie H, Peng Q, Zhu J. Progress in mechanic property and design theory of elementary structure of reactive powder concrete (RPC). Adv Mech. 2011;41(1):51-9.
- [5] De LF, Sedran T. Optimization of ultra-high-performance concrete by the use of a packing model. Cem Concr Res. 1994;24(6):997-1009.
- Yazici H. The effect of curing conditions on compressive strength of ultra high strength concrete with high volume mineral admixtures. Build Env. 2006;42(5):2083-9.
- Soutsos M, Millard S, Karaiskos K. Mix design, mechanical properties, and impact resistance of reactive powder concrete (RPC). International Workshop on High Performance Fibre-Reinforced Cementitious Composites in Structural Applications: 2005, p. 549-60.
- [8] Li S, Cheng S, Mo L, Deng M. Effects of steel slag powder and expansive agent on the properties of ultra-high performance concrete (UHPC): Based on a case study. Materials. 2020;13(3):683.
- Su J, Fang Z. Scale effect on cubic compressive strength of ordinary concrete and high-strength concrete. J Build Mater. 2013:16(6):1078-81.
- [10] Chen X, Wu S, Zhou J. Variability of compressive strength of concrete cores. J Perform Constr Facil. 2014;28(4):06014001.
- [11] Wang D, Shi C, Wu Z, Xiao J, Huang Z, Fang Z. A review on ultra high performance concrete: Part II. hydration, micro-structure and properties. Constr Build Mater. 2015;96:368-77.
- Roux N, Andrade C, Sanjuan MA. Experimental study of durability of reactive powder concretes. J Mater Civ Eng. 1996;8(1):1-6.
- Graybeal B. Material property characterization of ultra-high performance concrete. FHWA-HRT-06-103. United States: Federal Highway Administration. Department of Transportation; 2006. p. 176.
- [14] De Larrard F, Sedran T. Optimization of ultra-high-performance concrete by the use of a packing model. Cem Concr Res. 1994;24(6):997-1009.
- [15] Schmidt M, Fehling E. Ultra-high-performance concrete: Research, development and application in Europe. 7th International Symposium on Utilization of High Strength High Performance Concrete. Vol. 1; 2005. p. 51-77.
- [16] Vernet P. Ultra-durable concretes: Structure at the micro- and nano-scale. Mater Res Soc. 2004;29(5):324-7.
- Wille K, Naaman A, Montesinos G. Ultra-high performance concrete with compressive strength exceeding 150 MPa (22 ksi): A simpler way. ACI Mater J. 2011;108(1):46-54.
- [18] Li ZH, Xu K, Wei F. Recent progress in photodetectors based on low-dimensional nanomaterials. Nanotechnol Rev. 2018;7(5):393-411.
- [19] Pawłowski R, Pawłowski B, Wita H, Pluta A, Sobik P, Sala A, et al. Silver nanoparticles in the thermal silver plating of aluminium busbar joints. Nanotechnol Rev. 2018;7(5):365-72.
- Zhang HL. Selective modification of inner surface of halloysite nanotubes: A review. Nanotechnol Rev. 2017;6(6):573-81.
- Lin Q, Chen Y, Liu C. Mechanical properties of circular nano-[21] silica concrete filled stainless steel tube stub columns after being exposed to freezing and thawing. Nanotechnol Rev.
- [22] Genedy M. A new CFRP-UHPC system for strengthening reinforced concrete T-beams. Department of Energy. UNM's Digital Repository; 2014.

- [23] Katrin H, Emmanuel D, Eugen B. Experimental investigation of composite ultra high-performance fiber-reinforced concrete and conventional concrete members. Struct J. 2007;104:93-101.
- [24] Prem PR, Ramachandra Murthy A, Ramesh G, Bharatkumar BH, Iyer NR. Flexural behaviour of damaged RC beams strengthened with ultra high performance concrete. In: Matsagar V, editor. Advances in Structural Engineering. Springer; 2015. p. 2057–69.
- [25] Lampropoulos AP, Paschalis SA, Tsioulou OT, Dritsos SE. Strengthening of reinforced concrete beams using ultra high performance fibre reinforced concrete (UHPFRC). Eng Struct. 2016:106:370–84.
- [26] Al-Osta MA, Isa MN, Baluch MH, Rahman MK. Flexural behavior of reinforced concrete beams strengthened with ultra-high performance fiber reinforced concrete. Constr Build Mater. 2017:134:279–96.
- [27] Beschi C, Meda A, Riva P. Column and joint retrofitting with high performance fiber reinforced concrete jacketing. Appl Mech Mater. 2011;82(7):989-1014.
- [28] Lee MG, Huang YS. Fire-Damage or freeze-thaw of strengthening concrete using ultra high performance concrete. Adv Mater Res. 2009;79–82:2047–50.
- [29] Tayeh BA, Bakar BHA, Johari MAM, Voo YL. Mechanical and permeability properties of the interface between normal concrete substrate and ultra high performance fiber concrete overlay. Constr Build Mater. 2012;36:538–48.
- [30] Huang K, Xie J, Wang R, Feng Y, Rao R. Effects of the combined usage of nanomaterials and steel fibres on the workability, compressive strength, and microstructure of ultra-high performance concrete. Nanotechnol Rev. 2021;10(1):304–17.
- [31] Luo Q, Wu Y, Qiu W, Huang H, Pei S, Lambert P, et al. Improving flexural strength of UHPC with sustainably synthesized graphene oxide. Nanotechnol Rev. 2021;10(1):754-67.
- [32] Liu C, He X, Deng X, Wu Y, Zheng Z, Liu J, et al. Application of nanomaterials in ultra-high performance concrete: A review. Nanotechnol Rev. 2020;9(1):1427-44.
- [33] Bonneau O, Lachemi M, Dallaire E, Dugat J, Aitcin P. Mechanical properties and durability of two industrial reactive powder concretes. ACI Mater J. 1997;94(4):286–90.

- [34] Reda M, Shrive G, Gillott E. Microstructural investigation of innovative UHPC. Cem Concr Res. 1999;29(3):323-9.
- [35] Schmidt M, Fehling E, Teichmann T, Bunje K, Bornemann R. Ultra-high performance concrete: Perspective for the precast concrete industry. Concr Pre-Casting Plant Technol. 2003;69(3):16-29.
- [36] Herold G, Muller H. Measurement of porosity of ultra-high strength fibre-reinforced concrete. Proceedings of the International Symposium on Ultra-High Performance Concrete; 2004. p. 685–94.
- [37] Jun P, Taek K, Tae K, Wook K. Influence of the ingredients on the compressive strength of UHPC as a fundamental study to optimize the mixing proportion. Proceedings of the 2nd International Symposium on ultra High Performance Concrete; 2008. p. 105–12.
- [38] Ma DY, Han LH, Li W, Hou C, Mu TM. Behaviour of concreteencased CFST stub columns subjected to long-term sustained loading. J Constr Steel Res. 2018;151:58-69.
- [39] Graybeal B, Davis M. Cylinder or cube: Strength testing of 80–200 MPa (11.6–29 ksi) ultra high performance fibre-reinforced concrete. ACI Mater J. 2008;105(6):603–9.
- [40] Bayard O, Ple O. Fracture mechanics of reactive powder concrete: Material modeling and experimental investigations. Eng Fract Mech. 2003;70(7-8):839-51.
- [41] Zhang XY, Xia C, Chen Y. Research on nano-concrete-filled steel tubular columns with end plates after lateral impact. Rev Adv Mater Sci. 2021;60(1):553-66.
- [42] Poon CS, Shui ZH, Lam L. Compressive behavior of fiber reinforced high performance concrete subjected to elevated temperatures. Cem Concr Res. 2004;34(12):2215–22.
- [43] Taerwe L, AVan G. Influence of steel fibers on design stressstrain curve for high strength concrete. J Eng Mech. 1996;122:695–704.
- [44] Nataraja MC, Dhang N, Gupta AP. Stress-strain curves for steel-fiber reinforced concrete under compression. Cem Concr Compos. 1999;21:383–90.
- [45] Xiaoyong Z, Shihan C, Zhouhua W, Huiyun Q, Guixing L, Xiaolei W, Yu C. Research on mechanical properties of ultra-high performance fiber reinforced cement-based composite after elevated temperature. Compos Struct. 2022;291:115584.